



RESEARCH PAPER

OPEN ACCESS

Flood simulation using geospatial and hydrologic models in Manupali Watershed, Bukidnon, Philippines

George R. Puno^{*1}, Rose Angelica L. Amper², Bryan Allan M. Talisay²

¹College of Forestry and Environmental Science, Central Mindanao University, Musuan, Bukidnon, Philippines

²Center for Geomatics Research and Development in Mindanao, College of Forestry and Environmental Science, Central Mindanao University, Musuan, Bukidnon, Philippines

Article published on March 30, 2018

Key words: Disaster, Flood hazard, GIS, LiDAR.

Abstract

Application of geographic information system (GIS) and Hydrologic Engineering Center's (HEC) Hydrologic Modeling System and River Analysis System model using light detection and ranging (LiDAR)-derived digital elevation model (DEM) dataset to simulate floods at different return periods was conducted. The developed model for Manupali Watershed in Bukidnon, Philippines was calibrated using the May 23, 2016, flood event. The overall model performance was good with 0.65, 18.96, and 0.59 for the root Nash-Sutcliffe efficiency, percent bias, and root mean square error statistics, respectively. The simulated discharge and rainfall intensity duration frequency data were used to simulate flood events for 5-, 25- and 100-year return periods. Flood hazard maps generated within the GIS environment were classified into three different level depths corresponding to low, medium and high, respectively. Maps were validated through interviews and focus group discussions with the localities. The used of LiDAR datasets with hydrologic and GIS models able to generate high resolution and updated flood hazard maps useful in making more precise decisions and actions relative to disaster risk reduction management and mitigation.

*Corresponding Author: George R. Puno ✉ punogeorge@gmail.com

Introduction

Typhoons are now regarded as the new normal in Philippine climate (Tebtebba, 2013). Associated with typhoons are inundation along floodplains in most riverine systems in the country including Manupali River in Mindanao Philippines. With the desire of reducing risk, the government has mandated to prioritize research relative to climate change and natural disasters. Research efforts had been initiated to assess impacts in areas prone to flood hazards.

One of the most recognized techniques of assessing flood risk and vulnerability is through flood simulation, modeling and mapping (Glas, 2017; Tsanakas *et al.*, 2016; Puno and Amper, 2016; Romanowicz and Kiczko, 2016; Santillan *et al.*, 2016; Jung *et al.*, 2015; Roy *et al.*, 2013; Wang *et al.*, 2012; Suriya *et al.*, 2011; Yuan and Qaiser, 2011; El Bastawesy *et al.*, 2009; Valeriano *et al.*, Patro *et al.*, 2009; Mason *et al.*, 2007; Tingsanchali and Karim, 2005). Flood hazard simulation and mapping with hydrologic and geographic information systems (GIS) models using digital elevation model (DEM) are now commonly applied as the primary steps in vulnerability and risk assessment (Dewan, 2013; Mayomi *et al.*, 2013). However, there have been several issues regarding the uncertainty in flood modeling and mapping of which among of the probable causes is the techniques used in the process (Merwade *et al.*, 2008).

The accuracy and quality of data on ground elevation as well as the geometry of the modeled river have a remarkable impact upon flood mapping (Alho, 2009). Vozinaki *et al.*, (2016) speculated the advantage of highly accurate results of flood modeling in facilitating the effective management of extreme events. The choice of digital elevation model datasets is critical particularly in floodplain boundary delineation and consequently the simulated outputs (Di Luzio *et al.*, 2005). It is in this context that the use of LiDAR-derived DEM is advantageous due to its inherent high vertical accuracy and resolution which capture the details of the modeled terrain taking into account the correctness of the techniques applied during LiDAR-DEM data pre-processing (Lindsay and Dhum, 2014).

The inherent accuracy of LiDAR datasets makes it very appropriate input in flood simulation and mapping using GIS and hydrologic models.

The U.S. Army Corps of Hydrologic Engineers' HEC-HMS and HEC-RAS models are among the widely used tools in analyzing watershed hydrologic behaviors (Chatterjee *et al.*, 2014; Zope *et al.*, 2015). These computer programs provide current or future runoff information such as volumes, peak flow rates, and its timing through simulations in a hydrologic system and perform precipitation-runoff analysis and hydraulics. Such information will provide a significant contribution to the applications of flood forecasting and simulation of hydrological processes (Arekhi, 2012) as well as to the generation of flood hazard maps developed from the simulated water inundations.

The use of LiDAR data in flood mapping is gaining wide recognition due to its highly accurate and detailed digital georeferenced data sets. Its applicability extends to a wide array of mapping systems enabling specialists to examine natural or built surface characteristics with greater accuracy, precision, and flexibility (NOAA, 2012). LiDAR has been successfully applied in flood simulation and mapping for flood risk assessment in many regions of the Philippines (Puno *et al.* 2016; Puno and Barro, 2016). Using the combined technologies of HEC-HMS, HEC-RAS, GIS and the LiDAR-derived DEM, this paper illustrates the simulation and mapping of flood events along the floodplain of Manupali Watershed in Mindanao, Philippines. Specifically, the study aimed to develop HMS basin model; simulate floods for three return periods; and generate high-resolution flood hazard maps of the modeled site.

Materials and methods

Study Site

Having an average elevation of 1,270 meters above sea level, Manupali Watershed is geographically located between 7°58'38.93" to 8°13'50.16" North latitudes and 124°55'7.81" to 125°14'26.85" East longitudes with a total land area of 505.3km² (Fig. 1).

The soils of Manupali Watershed are mostly volcanic in origin. Clay materials forming minerals identified in the soil were halloysite, gibbsite, goethite, hematite, and cristobalite (Deharme-Calalang and Colinet, 2014). Generally, the soil is brown to dark brown, with a fine to medium granular structure and a very friable to friable moist consistency. Subsurface horizons were a brown to reddish color with a weak to moderate sub-angular blocky structure with slightly sticky and slightly plastic moist consistency having high water retention capacity (Deharme-Calalang and Colinet, 2014). The climate in the higher elevated portion (2,919 meters above sea level) of Manupali is characterized by short dry season with no pronounced rain period while in the lower portion (308 meters above sea level) has high relative humidity with rainy season which lasts for five to six months in a year (Rola *et al.*, 2004)

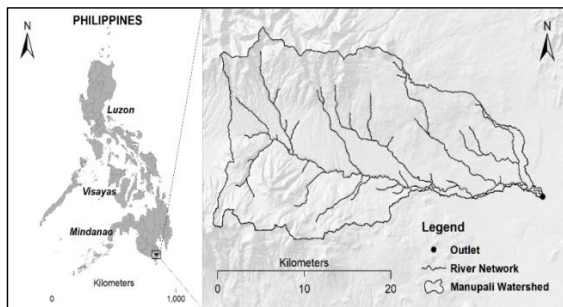


Fig. 1. Location map of Muleta Watershed.

Collection and Preparation of Datasets

Acquisition of LiDAR data was conducted using laser impulse emitting LiDAR sensors. Pre-process of such data able to generate Digital Elevation Model (DEM). Editing process includes filling the gaps of the DEM from the data gaps of flight mission; the interpolation which was done by omitting unnecessary objects and structures from DEM to stabilize changes in elevation; and the Object Retrieval which involves filling of accidentally omitted objects during the previous processes.

Quality checking and mosaicking of the different adjacent flight missions were conducted. Transitioning of overlapping DEM were interpolated and smoothed. Final DEM data with a vertical accuracy of $\pm 25\text{cm}$ and a resolution of 1m was used as the main input for flood simulation and mapping.

Feature extraction

Ground features referring to buildings and other built-up structures were extracted from the digital surface model (DSM), one of the processed output of LiDAR data. DSM, compared to digital terrain model (DTM), prominently shows roof features from the surveyed ground. Features were saved as polygons and attributed according to major categories of buildings. This was overlaid with the simulated flood hazards for the geospatial analysis of affected built-up structures.

Hydrologic Measurements

Precipitation and discharge data were collected needed to run HMS simulation. Precipitation data were collected using automatic rain gauge (ARG). River discharge was calculated using the data from the cross section, river stage and river velocity. River stage was obtained by tying up the water surface elevation to water level change which was determined using a deployed digital depth gauge. River velocity was measured at a gauging station at the lower portion of the river using a digital flow meter.

Bathymetric Survey

Bathymetric survey was conducted to fill the gaps of LiDAR DEM along the river bodies not penetrated by the laser lights during the LiDAR data acquisition. The process consisted of collecting coordinate and elevation points across and along the center line of the river. The collected points were tied up with the mean sea level for fix elevation reference of the river bed. The points were incorporated to LiDAR DEM through bathymetry burning.

A separate river cross-section survey extending approximately 50 meters from both sides of the reach was also conducted needed for the calculation of water discharge. Differential Global Positioning System (DGPS) surveying utilizing post process kinematic (PPK) technique was used in the survey. A single beam echo sounder was used in deeper portions of the river.

HMS Basin Model Generation

The main and subwatersheds boundaries of the Manupali Watershed model were generated using synthetic aperture radar (SAR) 10-m DEM.

The digitized river centerlines were digitized based on the extracted image from Google Earth. This serves as the most significant input for running the model for precipitation-runoff simulation over the entire watershed (Majidi and Shahedi, 2012).

Model Calibration and Evaluation

The process of calibration was done through manual adjustment and estimation of the parameters under the different models used in HEC-HMS (Choudhari, 2014). The different models used were the Soil Conservation Service (SCS) for loss method, Clark Unite Hydrograph (UH) for direct runoff, Recession for baseflow and Muskingum-Cunge for channel routing method. Model performance to simulate flooding event was evaluated by calculating the efficiency criteria such as the Nash-Sutcliffe efficiency (NSE), the ratio of the root mean square error to the standard deviation of measured data (RSR), and percent bias (PBIAS) as described in Moriase *et al.*, (2007). NSE is a test of model performance which indicates how well the plot of observed versus simulated data fits the 1:1 line. NSE ranges between ∞ and 1.0 (1 inclusive), with NSE = 1 being the optimal value (Leong, 2017). Values between 0.0 and 1.0 are generally viewed as acceptable levels of performance, whereas values <0.0 indicates that the mean observed value is a better predictor than the simulated value, which indicates unacceptable performance (Moriase, 2007). NSE is computed as shown below;

$$NSE = 1 - \left[\frac{\sum_{i=1}^n (Y_i^o - Y_i^s)^2}{\sum_{i=1}^n (Y_i^o - Y_i^m)^2} \right] \quad (1)$$

where Y_i^o is the i^{th} observation for the constituent being evaluated, Y_i^s is the i^{th} simulated value for the constituent being evaluated, Y_i^m is the mean of observed data for the constituent being evaluated, and n is the total number of observations. The RMSE-observations standard deviation ratio (RSR) standardizes RMSE using the observations standard deviation and incorporates the benefits of error index statistics and includes a scaling/normalization factor (Legates and McCabe, 1999). It ranges from the optimal value of 0 which indicates a perfect prediction or zero RMSE to large positive value.

It follows the lower RSR, the lower the RMSE, the better the model simulation performance (Moriase *et al.*, 2007). Using the symbols from the previous equation, RSR is calculated as the ratio of the RMSE and standard deviation shown in the below equation;

$$RSR = \frac{RMSE}{STDEV_o} = \frac{\left[\sqrt{\sum_{i=1}^n (Y_i^o - Y_i^s)^2} \right]}{\left[\sqrt{\sum_{i=1}^n (Y_i^o - Y_i^m)^2} \right]} \quad (2)$$

Percent bias (PBIAS) is another test of model performance which assesses the average tendency of the predicted results to overestimate or underestimate the field observed data (Setegn, 2010; Gupta *et al.*, 1999). A PBIAS of 0.0 indicates an accurate model performance. A positive value, on the other hand, indicates underestimation and overestimation if negative values (Gupta *et al.*, 1999). PBIAS of 55% of sediment modeling is already a satisfactory result (Moriase *et al.*, 2007). PBIAS is calculated with the equation below;

$$PBIAS = \left[\frac{\sum_{i=1}^n (Y_i^o - Y_i^s) 100}{\sum_{i=1}^n Y_i^o} \right], \quad (3)$$

where symbols are described from previous equations.

Scenario-based Simulations Using RIDF

Three different return period scenarios (5-year, 25-year, and 100-year) were simulated based on Rainfall Intensity Duration Frequency (RIDF) obtained from the Philippines Atmospheric Geophysical and Astronomical Services Administration (PAGASA). Precipitation depths of each return period in specific durations are inputted in separate meteorological models created for each return period through the frequency storm method.

HEC-RAS Model Development and Simulation

The method employed in Santillan *et al.*, (2016) was followed in creating a 2D hydraulic model of Manupali River using the Hydrologic Engineering Center River Analysis System (HEC RAS) version 5.0, which is designed to perform one-dimensional (1D), two-dimensional (2D), or combined 1D and 2D hydraulic calculations for a full network of natural and constructed channels (USACE 2016).

The geometric data was developed in ArcGIS using the HEC-geoRAS extension toolbars. RAS layers namely the storage area and break lines were created which serve as the two-dimensional (2D) model domain or floodplain area and the representation for abrupt changes in elevation like banks, roads and levees, respectively. The layers were imported to HEC-RAS for the creation of 2D flow area and calculated computational mesh together with the break lines.

The 1-m resolution terrain model was used as the primary source of elevation data. Parameterization of the HEC-RAS model utilized the land cover information by extracting the Manning's roughness coefficients, and these values were used to calculate the hydraulic table properties of computational mesh. The model consisted of two boundary conditions in which one for the inflow from upstream rivers and one for the friction slope at the downstream portion as inputs into the HEC-RAS 2D hydraulic model to predict or estimate flood depths and extents. The inflow represents the flow of water or the hydrographs that enters the 2D model domain. The simulated discharge from three different return periods were used as an input in the inflow with unsteady flow analysis module to dynamically simulate depth and extent of flooding. For each return period flood simulation, a spatially-distributed grid of maximum flood depths was created. The depth grid was then exported as a raster file in the GIS environment and converted into flood hazards by categorizing depths to its corresponding flood hazard levels (Low Hazard: less than 0.50 m, Medium Hazard: 0.50 m to 1.50 m, and High Hazard: greater than 1.50m).

Results and discussion

HMS Basin Model

The HEC-HMS basin model of Manupali Watershed (Fig. 2) has a total 26 subwatershed with 13 reaches and 14 junctions. A hydrologic model is required for runoff generation from precipitation, transformation, and combination with baseflow, and routing towards the outlet.

Methods used for each component were the following: US Soil Conservation Service-Curve Number (US SCS-CN) method for infiltration loss model, Clark Unit Hydrograph for direct runoff model, Exponential Recession for baseflow, and Muskingum-Cunge Standard for Channel routing. These components comprise the set of equations that helped in the estimation of runoff (Devi *et al.*, 2015). Computation CN parameter of SCS-CN infiltration loss component was accomplished using soil and land cover maps.

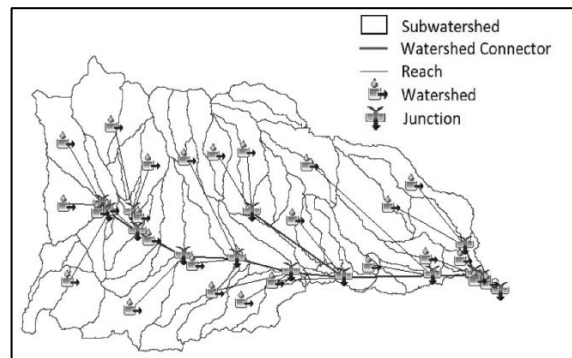


Fig. 2. HMS watershed model of Manupali Watershed.

Discharge and precipitation data of the actual event on May 23, 2016, was utilized for the initial precipitation-runoff simulation of HEC-HMS model. Total precipitation amount recorded using automatic rain gauge from PAGASA was 130.4mm (Fig. 3). It peaked to 25.4 mm on 23 May 2016 at around 17:30. Gathered discharge data began at 13:20 of 23 May 2016 to 10:10 on 24 May 2016. Peak discharged recorded at 11.03m³/s on the first day at around 21:40. The lag time between the peak precipitation and discharge was 4 hours and 10 minutes.

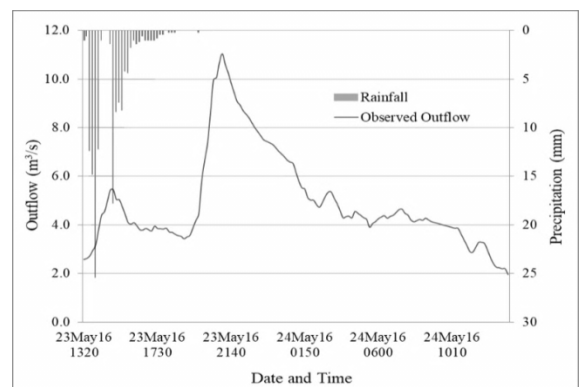


Fig. 3. Hydrograph for observed rainfall and outflow data.

HMS Model Calibration and Evaluation

Calibration was conducted to fit the hydrographs of the simulated and the actual outflows. The progress of calibration was inspected through visual comparison between the observed and simulated hydrographs. This approach is considered as one of the most fundamental in assessing model performance (Krause, 2005). (Fig. 4) shows the comparison between the observed and simulated outflows in cubic meters per second. Model performance testing was done using appropriate statistical tools after calibration. As shown in Table 1, the overall performance test results of the model were found good with the reduction of the overestimated values of the default simulation indicating acceptability of the model and the appropriateness of LiDAR dataset to be used in simulating and mapping flood hazard maps in the area.

Table 1. Model performance evaluation results.

Statistical Tools	Values	Rating
NSE	0.65	Good
RSR	18.96	Satisfactory
PBIAS	0.59	Good

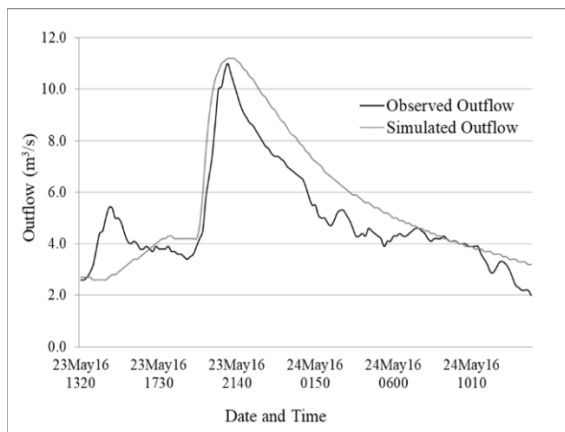


Fig. 4. Hydrograph of the simulated outflows used in flood mapping for three scenarios.

Discharge Simulation for Three Return Period Using RIDF Data

Calibrated HMS model was utilized for the simulation of rainfall events using the RIDF data of PAG-ASA. The precipitation depths of three different return periods based on long historical data and the simulated hydrographs are shown in Fig. 5.

The return period is the occurrence interval of an event equivalent to 20, 4 and 1% for 5-, 25- and 100-year return periods, respectively. These values can be used as basic information for early warning of the expected future flooding events so that the local government unit and or the community may have prior knowledge to the frequency and probability of flood-related disaster occurrences.

The simulated precipitation depth values for the 5-, 25- and 100-year return period scenarios were 26.70mm, 39.9mm, and 50.8mm, respectively. These depths revealed peak flows of 258.7m³s⁻¹, 657m³s⁻¹, and 1101.9m³s⁻¹, respectively. Results show that discharge from 5-, 25-year and from 25- to 100-year return period scenarios had increased by about 60% and 40.4%, respectively.

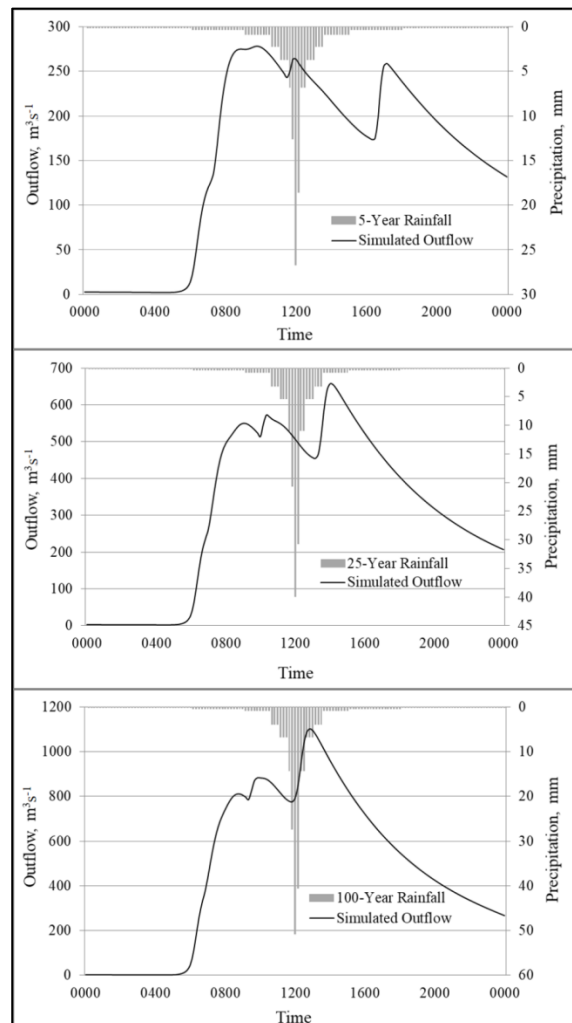


Fig. 5. Hydrograph for 5-, 25-, and 100-year return periods using RIDF data.

Flood Hazard Mapping

Simulated flood events were categorized into 3 flood hazard indices according to flood depth ranging from 0 - 0.5m, 0.5 - 1.5m, and more than 1.5m as low, medium and high, respectively (Fig. 6). The 5-year return period illustrates the wider extent of inundation covering several residential houses in the area. Flood hazard for the 25-year and 100-year return periods have an increasing coverage of flood inundation with highest hazard category of medium affecting other several residential houses. Overlaid extracted features from the LiDAR DSM revealed 2 affected built-up structures identified as the commercial establishment and residential for the 5-year return period scenario. This scenario implies a 20% probability to occur in the area in a year as based on the historical rainfall data or RIDF. For the 25-year return period scenario which corresponds to 4% probability of occurring in a year revealed around 22 affected built-up structures, 18 of which are identified as commercial establishment while four were residential houses. The 100-year return period scenario with 1% probability of occurring in a year shows a total of 34 flooded buildings, 18 of which were commercial establishments while 16 were domestic houses.

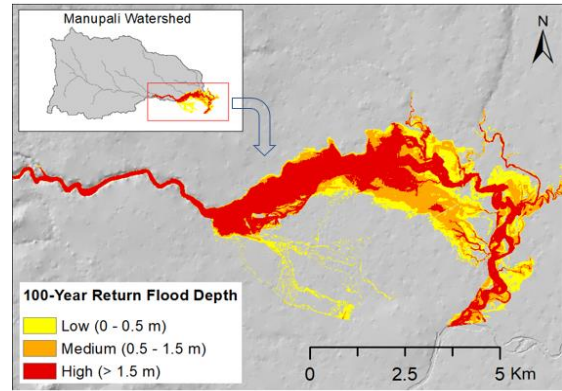
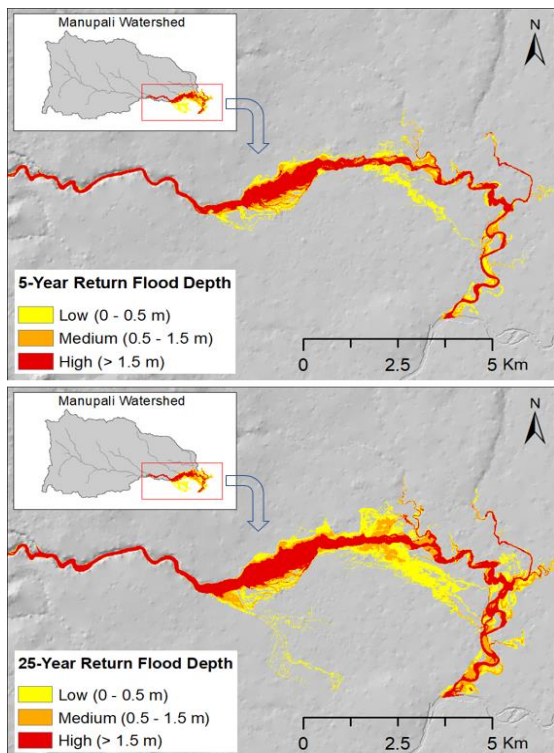


Fig. 6. Flood hazard maps for the three return period scenarios.

Conclusion

A developed hydrologic model of Manupali River basin was used for precipitation and discharge simulations. The model was calibrated using the 23rd May 2016 event. Through manual adjustment of parameters, the model was evaluated using the statistical evaluation techniques of NSE, RSR and PBIAS obtaining an overall satisfactory performance. Using the calibrated model, three different return periods were simulated and the corresponding flood hazard maps were generated using GIS and LiDAR-derived DEM. Resulting hazard map revealed bank overflows at certain areas of the modeled site. The generated map was validated through an interview with the affected localities.

Simulation results of 5-year, 25-year and 100-year return periods using RIDF data revealed inundations in the same areas. Field validation of the generated flood hazard maps using LiDAR-derived DEM was confirmed by the affected communities with a certain level of accuracy implying the advantage of using LiDAR-derived DEM in flood modeling and mapping. Results indicate the applicability of both developed HMS and HEC-RAS models in performing flood simulations with GIS and LiDAR-derived DEM. Validated high resolution and updated flood hazard maps with a certain level of precision are important to government officials in arriving at a more science-based law and policies so that decisions and actions relative to the implementation of disaster risk reduction management programs and the project can be more efficient and cost-effective.

Acknowledgements

The authors would like to thank the following: to the CMU Administration and its constituents for the support in the implementation of the project entitled "Project 11. LiDAR Data Processing and Validation in Mindanao: Regions 10, 12 and ARM1" where this study was conducted; to the Philippine Council for Industry, Energy and Emerging Technology Research and Development-Department of Science and Technology (PCIEERD-DOST) for the funding support.

References

- Alho P, Hyypä H, Hyypä J.** 2009. Consequences of DEM precision for flood hazard mapping: a case study in SW Finland. *Nordic Journal of Surveying and Real Research* **6(1)**, 21-39.
- Arekhi S.** 2012. Runoff modeling by HEC-HMS model (case study: Kan watershed, Iran). *International Journal of Agriculture and Crop Sciences* www.ijagcs.com. Accessed 21 September 2017.
- Chatterjee M, De R, Roy D, Das S, Mazumdar A.** 2014. Hydrological modeling studies with HEC-HMS for Damodar basin, India. *IDOSI Publications. World Applied Sciences Journal* **31**, 2148-2154. www.researchgate.net/publication/262914536. Accessed 21 September 2017.
- Choudhari K, Panigrahi B, Paul JC.** 2014. Simulation of the precipitation-runoff process using HEC-HMS model for Balijore Nala watershed, Odisha, India. *International Journal of Geomatics and Geosciences* **5(2)**, 253-265.
- Deharme-Calalang GM, Colinet G.** 2014. A review of soils and crops in the Bukidnon Highlands of Northern Mindanao, the Philippines. *Biotechnology, Agronomy, Society and Environment* **18(4)**, 544-557.
- Devi GK, Ganasri BP, Dwarakish GS.** 2015. A Review on hydrological Models. In: *International Conference on Water Resources, Coastal and Ocean Engineering. Aquatic Procedia* **4**, 1001-1007.
- Dewan AM.** 2013. *Floods in a Megacity: Geospatial Techniques in Assessing Hazards, Risk and Vulnerability*. Springer Dordrecht Heidelberg New York London.
- Di Luzio M, Arnold JG, Srinivasan R.** 2005. Effects of GIS data quality on small watershed stream flow and sediment simulations. *Hydrological Processes* **19(3)**, 629-650.
- El Bastawesy M, White K, Nasr A.** 2009. Integration of remote sensing and GIS for modeling floods in Wadi Hudian catchment, Egypt. *Hydrological Processes* **23**, 1359-1368.
- Glas H, Jonckheere M, Mandal A, James-Williamson S, De Maeyer P, Deruyter G.** 2017. A GIS-based tool for flood damage assessment and delineation of a methodology for future risk assessment: case study for Annotto Bay, Jamaica. *Natural Hazards* doi:10.1007/s11069-017-2920-5.
- Gupta HV, Sorooshian S, Yapo PO.** 1999. Status of automatic calibration for hydrologic models: Comparison with multilevel expert calibration. *Journal of Hydrologic Engineering* **4(2)**, 135-143.
- Jung Y, Merwade V.** 2015. Estimation of uncertainty propagation in flood inundation mapping using a 1-D hydrograph model. *Hydrological Processes* **29**, 624-640.
- Krause P, Boyle DP, Base F.** 2005. Comparison of different efficiency criteria for hydrological model assessment. *European Geosciences Union. Advances in Geosciences* **5**, 89-97.
- Legates DR, McCabe GJ.** 1999. Evaluating the use of "goodness-of-fit" measures in hydrologic and hydroclimatic model validation. *Water Resources* **35(1)**, 233-241.
- Leong WK, Lai SH.** 2017. Application of Water Evaluation and Planning Model for Integrated Water Resources Management: Case Study of Langat River Basin, Malaysia. *IOP Conference Series: Materials Science and Engineering* **210(1)**, 1-14.

- Lindsay JB, Dhun K.** 2015. Modelling surface drainage patterns in altered landscapes using LiDAR. *International Journal of Geographical Information Science* **29(3)**, 397-411.
- Majidi A, Shahedi K.** 2012. Simulation of precipitation-runoff process using green-ampt method and HEC-HMS model (Case Study: Abnama watershed, Iran). *International Journal of Hydraulic Engineering* **1(1)**, 5-9.
- Mason DC, Horritt MS, Hunter NM, Bates PD.** 2007. Use of fused airborne scanning laser altimetry and digital map data for urban flood modeling. *Hydrological Processes* **21(11)**, 1436-1447.
- Mayomi I, Dami A, Maryah UM.** 2013. GIS assessment of flood risk and vulnerability of communities in the floodplains, Adamawa State, Nigeria. *Journal of Geography and Geology* **5(4)**, 148-160.
- Merwade V, Ovivera F, Arabe M, Edleman S.** 2008. Uncertainty in flood inundation mapping: current issues and future directions. *Journal of Hydrology Engineering* **13(7)**, 608-620.
- Moriasi DN, Arnold JG, Van Liew MW, Bingner RL, Harmel RD, Veith TL.** 2007. Model Evaluation Guidelines for Systematic Quantification of Accuracy in Watershed Simulations. *American Society of Agricultural and Biological Engineers* **50(3)**, 885-900.
- NOAA.** 2012. National Oceanic and Atmospheric Administration, Coastal Services Center. Lidar 101: An Introduction to LiDAR Technology, Data, and Applications. Revised. Charleston, South Carolina, USA: NOAA Coastal Services Center.
- Patro S, Chatterjee C, Singh R, Raghuvanshi NS.** 2009. Hydrodynamic modeling of a large flood-prone river system in India with limited data. *Hydrological Processes* **23(19)**, 2774-2791.
- Puno GR, Amper RAL.** 2016. Flood modeling of Musimusi River in Balingasag, Misamis Oriental. *Central Mindanao University Journal of Science* **20(3)**, 150-165.
- Puno GR, Barro RI.** 2016. Alubijid river basin hydrologic modeling in Misamis Oriental for flood risk management. *Central Mindanao University Journal of Science* **20(3)**, 97-106.
- Puno GR, Talisay BAM, Paquit JC.** 2016. GIS-Based flood hazard mapping in Gingoog River, Mindanao. *Central Mindanao University Journal of Science* **20(3)**, 81-96.
- Rola AC, Sumbalan AT, Suminguit VJ.** 2004. Realities of the Watershed Management Approach: The Manupali Watershed Experience. Discussion Paper Series No. 2004-23. Philippine Institute for Development Studies.
- Romanowicz RJ, Kiczko A.** 2016. An event simulation approach to the assessment of flood level frequencies: risk maps for the Warsaw reach of the River Vistula. *Hydrological Processes*
DOI: 10.1002/hyp.10857.
- Roy D, Begam S, Ghosh S, Jana S.** 2013. Calibration and validation of HEC-HMS model for a river basin in eastern India. *Asian Research Publishing Network Journal of Engineering and Applied Sciences* **8(1)**, 40-56.
- Santillan JR, Amora AM, Makinano-Santillan M, Marqueso JT, Cutamora LC, Serviano JL, Makinano RM.** 2016. Assessing the impacts of flooding caused by extreme rainfall events through a combined geospatial and numerical modeling approach. *International Archive. Photogrammetry, Remote Sensing, Spatial Information Science XLI-B8: 1271-1278*,
www.doi.org/10.5194/isprs-archives-XLI-B8-1271-2016, 2016.
- Setegn SG, Dargahi B, Srinivasan R, Melesse AM.** 2010. Modeling of sediment yield from Anjeni-gauged Watershed, Ethiopia using SWAT model. *Journal of the American Water Resources Association* **46(3)**, 514-526.
- Suriya S, Mudgal BV, Nellyat P.** 2001. Flood damage assessment of an urban area in Chennai, India part I: methodology. *Natural Hazards* **62(2)**, 149-167.

- Tebtebba.** 2013. Coping with the “New Normal” in Philippine Climate. Indigenous Information Services. E-Newsletter. www.indigenousclimate.org.
- Tingsanchali T, Karim MF.** 2005. Flood hazard and risk analysis in the southwest region of Bangladesh. *Hydrological Processes* **19(10)**, 2055-2069.
- Tsanakas K, Gaki-Papanastassiou K, Kalogeropoulos K, Chalkias C, Katsafados P, Karymbalis E.** 2016. Investigation of flash flood natural causes of Xirolaki Torrent, Northern Greece based on GIS modeling and geomorphological analysis. *Natural Hazards*
DOI 10.1007/s11069-016-2471-1.
- USACE.** 2016. HEC-RAS River Analysis System Hydraulic Reference Manual, Institute for Water Resources Hydrologic Engineering Center, Davis, California, USA.
- Valeriano OCS, Koike T, Yang D, Thanda Nyunt C, Duong VK, Chau NL.** 2009. Flood simulation using different sources of rainfall in the Huong River, Vietnam. *Hydrological Sciences Journal* **54(5)**, 909-917.
- Vozinaki AEK, Morianou GG, Alexakis DD, Tsanis IK.** 2016. Comparing 1D- and combined 1D/2D hydraulic simulations using high-resolution topographic data, the case study of the Koiliaris basin, Greece. *Hydrological Sciences Journal* **62(4)**, 642-656.
- Wang W, Yang X, Yao T.** 2012. Evaluation of ASTER GDEM and SRTM and their suitability in hydraulic modeling of a glacial lake outburst flood in southeast Tibet. *Hydrological Processes* **26(2)**, 213-225.
- Yuan Y, Qaiser K.** 2011. Floodplain modeling in the Kansas River Basin using Hydrologic Engineering Center (HEC) models impacts of urbanization and wetlands for mitigation. U.S. Environmental Protection Agency, Office of Research and Development 2011 - 32 pages.
- Zope PE, Eldho TI, Jothiprakash V.** 2015. Impacts of urbanization on flooding of a coastal urban catchment: a case study of Mumbai City, India. *Natural Hazards* **75(1)**, 887-908.